

JOINT INSTITUTE FOR NUCLEAR RESEARCH  
Veksler and Baldin Laboratory of High Energy Physics

# FINAL REPORT ON THE SUMMER STUDENT PROGRAM

Study of Vortical structure in heavy-ion collisions

**Supervisor:** Dr. Oleg Teryaev, JINR

**Student:** Egor Alpatov, NRNU MEPhI

**Participation Period:** August 01 - September 14

Dubna, 2019

## Abstract

This work is dedicated to study of vortical structure of matter in heavy-ion collisions. Analysis of transport properties of Quark-Gluon Plasma (QGP) is very important in modern physics. In this research were obtained results of velocity, vorticity and helicity measurements with different hadron species. Performed comparison of different methods of calculation. For this analysis was generated data of Au+Au collisions with  $\sqrt{s_{NN}} = 11.5$  GeV by UrQMD model (Ultra-relativistic Quantum Molecular Dynamics).

Obtained results could be used in other QGP studies, like global polarization, chiral vortical effect (CVE), the chiral vortical wave (CVW) etq.

# Contents

<b>1. Introduction</b>	<b>4</b>
<b>2. Theory Overview</b>	<b>5</b>
2.1. Velocity and vorticity within hydrodynamics . . . . .	5
2.2. Helicity and global polarization . . . . .	5
<b>3. The UrQMD model</b>	<b>6</b>
3.1. Model description . . . . .	6
3.2. Simulation parameters and features . . . . .	6
<b>4. Vortical structure study</b>	<b>7</b>
4.1. Velocity and vorticity calculations . . . . .	7
4.2. Helicity separation and Global Polarization . . . . .	10
<b>5. Conclusion and Outlook</b>	<b>12</b>
<b>6. References</b>	<b>13</b>

# 1. Introduction

The extreme temperatures and energy densities generated by non-central collisions have angular momentum on the order of  $1000 \hbar$ , and the resulting fluid may have a strong vortical structure that must be understood to properly describe the fluid. Recently, it was realized that noncentral heavy-ion collisions can also generate finite flow vorticity and thus provide us with a chance to study quark-gluon matter under local rotation [1]. The mechanism of the generation of finite vorticity is simple[2].

In a non central heavy-ion collision, the two colliding nuclei have a finite angular momentum in the direction perpendicular to the reaction plane,  $J_0 = Ab\sqrt{s_{NN}}/2$ , with  $A$  the number of nucleons in one nucleus,  $b$  the impact parameter, and  $\sqrt{s_{NN}}$  the center-of-mass energy of a pair of colliding nucleons. After the collision, a fraction of the total angular momentum is retained in the produced partonic matter which we will call the quark-gluon plasma (QGP). This fraction of angular momentum manifests itself as a shear of the longitudinal momentum density and thus nonzero local vorticity arises. In hydrodynamics, the vorticity represents the local angular velocity, and its existence in heavy-ion collisions may induce a number of intriguing phenomena, for example, the chiral vortical effect (CVE) [3], the chiral vortical wave(CVW) [4], and the global polarization of quarks and  $\Lambda$  hyperons[5].

## 2. Theory Overview

### 2.1. Velocity and vorticity within hydrodynamics

In non-relativistic hydrodynamics, the fluid vorticity is defined by  $\omega = (1/2)\nabla \cdot \mathbf{v}$  with  $\mathbf{v}$  the flow velocity, which represents the local angular velocity of the fluid cell. In this analysis velocity of cell was defined as  $\langle \frac{p_i}{E_i} \rangle$ , where  $p_i, E_i$  are momentum and full energy of  $i$ -th particle inside cell.

The relativistic extension of  $\omega$  is not unique. One can define different relativistic vorticities according to different physical conditions. A natural one is the kinematic vorticity,  $\omega^\mu = (1/2)\epsilon^{\mu\nu\rho\sigma}u_\nu\partial_\rho u_\sigma$ , where  $u^\mu = \gamma(1, \mathbf{v})$  is the four velocity with  $\gamma = 1/\sqrt{1-v^2}$  being the Lorentz factor, whose spatial components reduce to the non-relativistic vorticity in low-velocity limit[6]. This definition of vorticity was used in this analysis.

### 2.2. Helicity and global polarization

Hydrodynamical helicity  $H = \int dV(\mathbf{v}\omega)$  is the pseudoscalar characteristics of the vorticity, which is related to a number of interesting phenomena in hydrodynamics and plasma physics, such as the turbulent dynamo and Lagrangian chaos[7].

In the other hand, helicity is the quantity, which gives information about global polarization of particles in collision. In non-central heavy-ion collisions, the created medium is supposed to have a large angular momentum transferred by two colliding nuclei. Such an initial angular momentum would be partially transferred to the spin of produced particles and then the resulting global polarization would be experimentally detectable via hyperons through their parity-violating weak decay.

One of methods of measuring polarization is based on the calculation of strange axial charge[8]:

$$Q_5^s = \frac{\langle \mu^2 \gamma^2 \rangle N_c H}{2\pi^2} \quad (1)$$

The average polarization can be estimated by dividing  $Q_5^s$  by the number of  $\Lambda$ 's, assuming that the pseudovector of axial current is proportional to the pseudovector of polarization  $Q_5^s \propto \Pi_0^{\Lambda, lab}$ . Selecting the axial charge related to the particles in the definite rapidity or transverse momentum interval, the respective dependence of polarization may be also obtained.

As the axial charge should be related to the zeroth component of hyperon polarization in laboratory frame  $\Pi_0^{lab}$ , the transformation to hyperon rest frame should be performed as follows:

$$\langle \Pi_0^\Lambda \rangle = Q_5^s \langle \frac{M_\Lambda}{N_\Lambda p_y} \rangle \quad (2)$$

## 3. The UrQMD model

### 3.1. Model description

The UrQMD is a microscopic transport model designed for the description of hadron-hadron ( $hh$ ), hadron-nucleus ( $hA$ ) and nucleus-nucleus ( $AA$ ) collisions for energies spanning a few hundred MeV up to hundreds of GeV per nucleon in the center-of-mass system (c.m.system). The model is presented in detail in [9, 10]. As discrete, quantized degrees of freedom, the model contains 55 baryon and 32 meson states, together with their antiparticles and explicit isospin-projected states, with masses up to  $2.25 \text{ GeV}/c^2$ . The tables of the experimentally available hadron cross sections, resonance widths and decay modes are implemented as well. At moderate energies the dynamics of  $hh$  or  $AA$  collisions is described in UrQMD in terms of interactions between the hadrons and their excited states (resonances). At higher values of the four-momentum transfer,  $hh$  interactions cannot be reduced to the hadron-resonance picture anymore, and new excited objects, color strings, come into play.

The excitation of the strings make it energetically favorable to break the string into pieces by producing multiple  $\bar{q}q$ -pairs from the vacuum. Due to the fact that the color string is assumed to be uniformly stretched, the hadrons produced as a result of the string fragmentation will be uniformly distributed in rapidity between the endpoints of the string. The propagation of the hadrons is governed by Hamilton equations of motion, with a binary collision term of the form of relativistic Boltzmann-Uehling-Uhlenbeck (BUU) transport model. The Pauli principle is taken into account via the blocking of the final state, if the outgoing phase space is occupied[11].

### 3.2. Simulation parameters and features

For this analysis was generated  $200 \times 10^3$  of Au+Au collisions with  $\sqrt{s_{NN}} = 11.5 \text{ GeV}$  at time = 15 fm/c after collision and with impact parameter from 0 to 9.

To make UrQMD data closer to hydrodynamic theory, all particles values were distributed in space by Gauss distribution with normalization to 1.

## 4. Vortical structure study

### 4.1. Velocity and vorticity calculations

For forward calculations coordinate space was divided into  $40 \times 40 \times 40$  cells of volume with  $dx=dy=dz=1$  fm. Particles values were distributed by Gaussian with  $\sigma$  parameter connected with distance to center of the nearest 5 cells in all directions.

The results of velocity calculations for impact parameter = 6 fm are presented below (Fig.1-3).

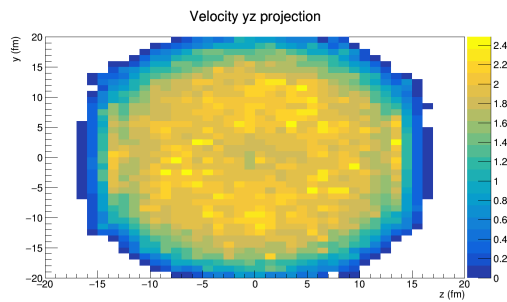


Figure 1. Velocity field projection on yz-plane

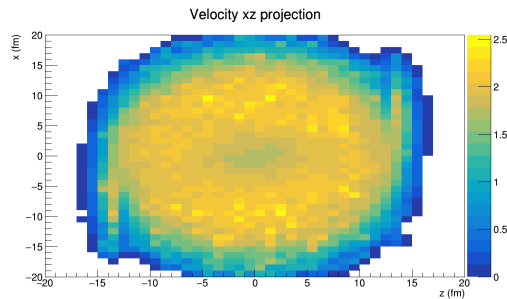


Figure 2. Velocity field projection on xz-plane

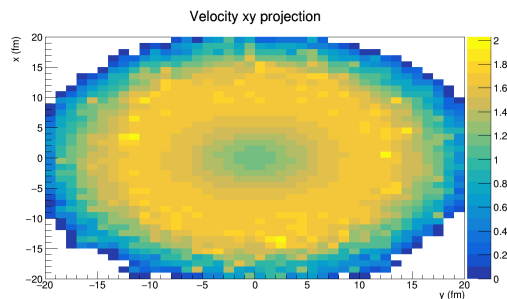


Figure 3. Velocity field projection on xy-plane

Velocities were calculated for three cases: for all particles in cell, only for baryons in cell and only for mesons in cell. These three different calculations gave different values of velocity (Fig.4). It's interesting to inspect this phenomena to understand fluid properties of matter. The ratio of different calculations to each other are presented on Figure 5.

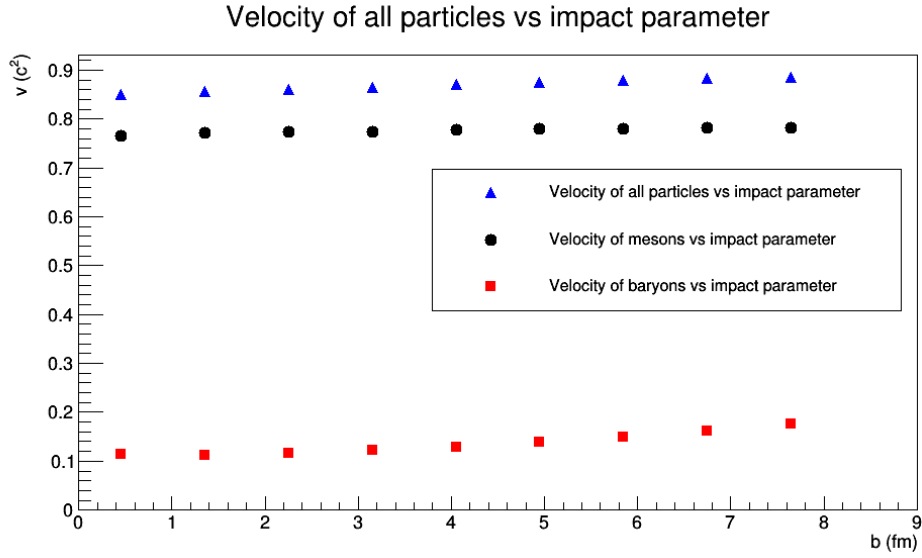


Figure 4. Mean velocities for different particles vs impact parameter

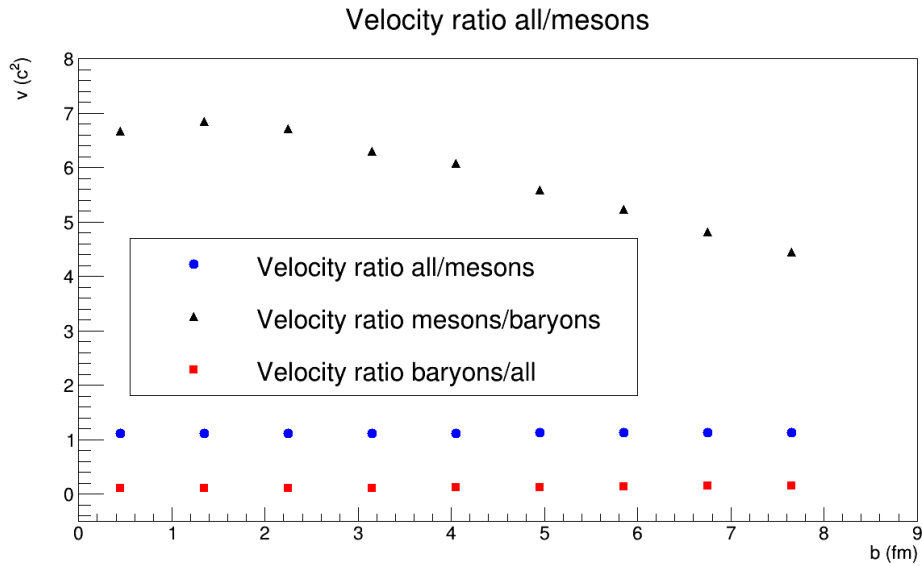


Figure 5. Ratio of different velocity calculations

As it seems, results for all particles and only for mesons are close, but there is big difference for baryons velocities. It means that there is division in fluid, that should be inspected in future. It is possible, that this phenomena is a manifestation of some superfluid properties of mesons component.

The same procedure was done for vorticity, and it gave the same result, except that difference between full-baryon and baryon-meson ratio become bigger (Fig.6). That happens, because vorticity is differential value and it is more sensible to fluctuations.

Below (Fig.7) is shown vorticity projection to xz plane with  $z = 0$ . It has quadruple-like structure in reaction plane. First and third quadrant are connected with central region which has small negative vorticity.

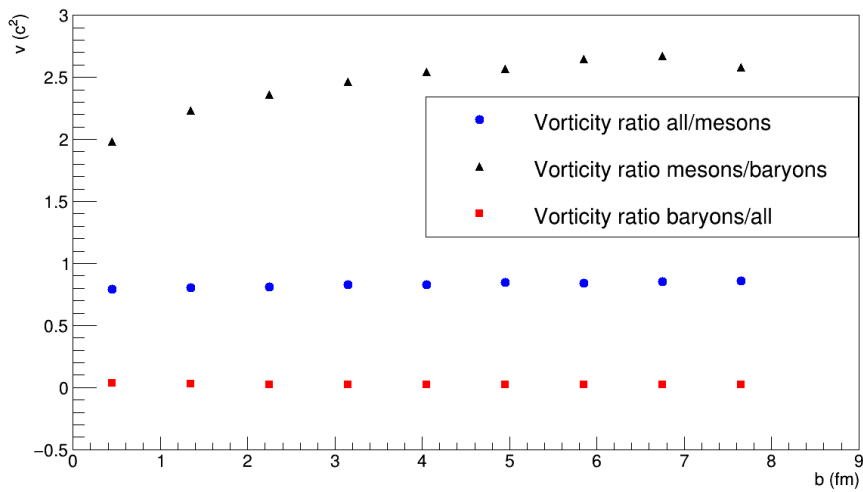


Figure 6. Ratio of different vorticity calculations

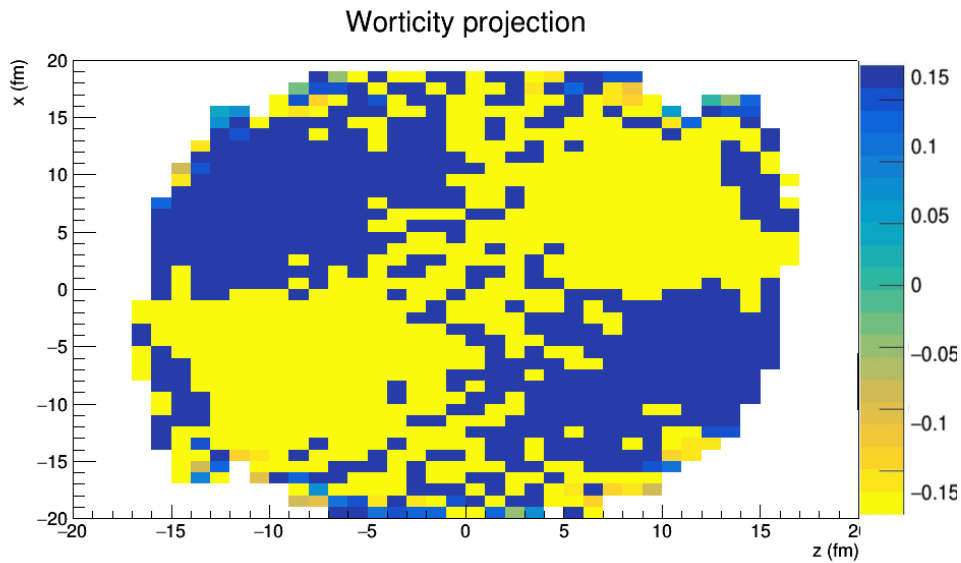


Figure 7. Vorticity in reaction plane

## 4.2. Helicity separation and Global Polarization

For each cell Helicity was calculated as a projection of velocity vector to vorticity vector. Then it was summarized around all cells. Observed result was mostly zero. For the cells with the definite sign of the velocity components, which are orthogonal to the reaction plane (which may be selected also experimentally), the helicity is nonzero and changes the sign for the different signs of these components (Fig.8). The effect is growing with impact parameter.

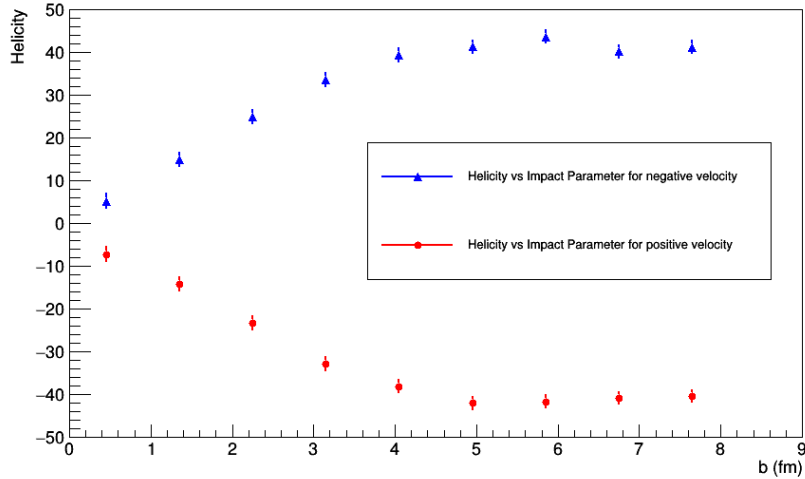


Figure 8. Helicity separation

Helicity was too calculated for mesons, baryons and all particles (Fig.9). As shown at Fig.10, this value is much more sensible for particles parameters. Ratios of full-baryon and meson-baryons have big difference, which means, that calculating polarization, using helicities from different particles wouldn't give the same result, and this interesting point should be inspected in future too.

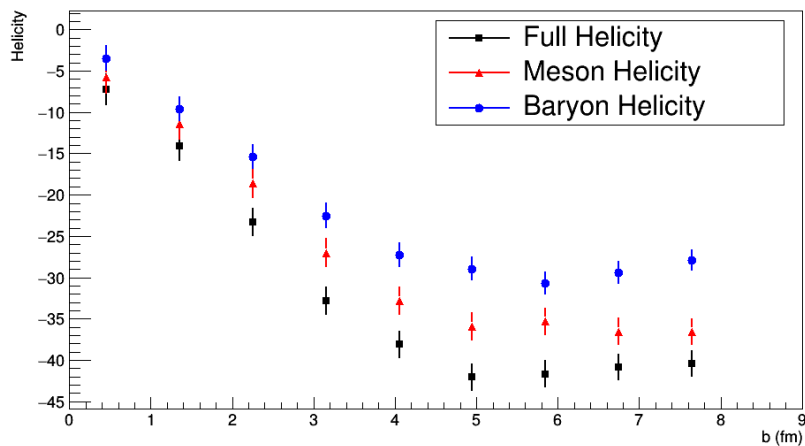


Figure 9. Mean helicity vs impact parameter

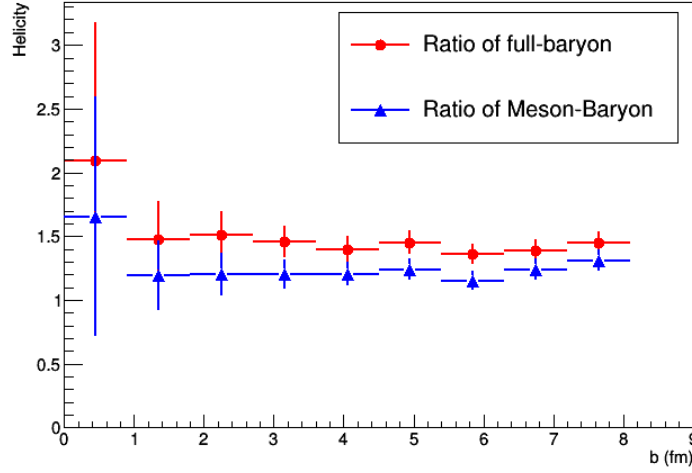


Figure 10. Helicity ratios for full-baryon and meson-baryon cases

Finally, using formulas (1),(2) global polarization of  $\Lambda$  hyperons was obtained. Chemical potential of strange quark  $\mu$  was taken 30 MeV. Polarization was calculated, as helicity, for cases with  $y \geq 0$  and  $y < 0$ . Results are shown on Fig. 11.

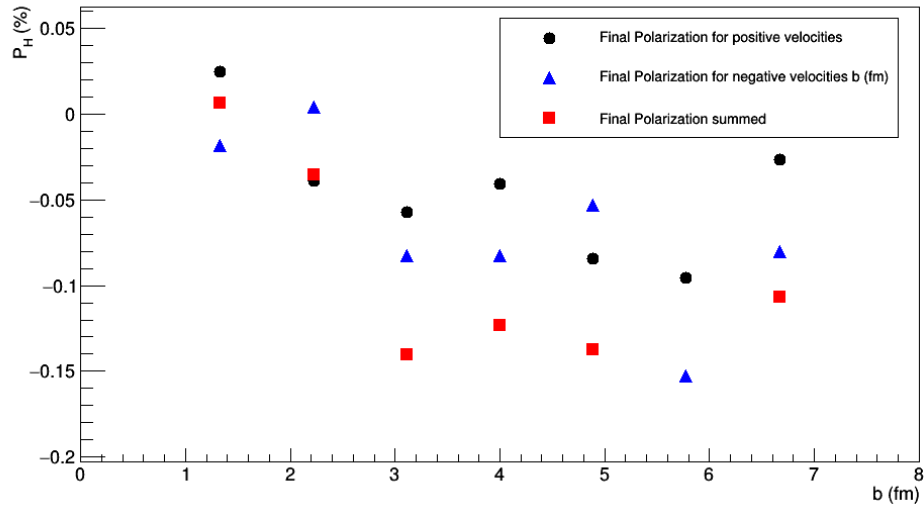


Figure 11. Polarization for different  $y$  sign vs impact parameter

## 5. Conclusion and Outlook

During analysis were investigated following physical quantities within UrQMD model: velocity, vorticity and hydrodynamical helicity. All values were calculated for all particles, baryons and mesons.

Observed difference in ratios for all quantities, what is giving information about non-uniform structure of fluid, what could be understood in superfluid theory. The influence of this effect should be investigated in future.

In analysis were shown quadruple-like structure of vorticity in reaction plane and helicity separation due velocity sign changes.

At least global  $\Lambda$  polarization signal dependence from impact parameter was obtained.

## 6. References

### References

- [1] L. P. Csernai, V. K. Magas and D. J. Wang, Phys. Rev. C87(2013), 034906 [arXiv:1302.5310 [nucl-th]].
- [2] Wei-Tian Deng and Xu-Guang Huang 2017 J. Phys.: Conf. Ser.779 012070
- [3] D. E. Kharzeev, J. Liao, S. A. Voloshin and G. Wang, Prog. Part. Nucl. Phys.88(2016), 1 [arXiv:1511.04050 [hep-ph]].
- [4] Y. Jiang, X. G. Huang and J. Liao, Phys. Rev. D92(2015), 071501 [arXiv:1504.03201 [hep-ph]]
- [5] Z. T. Liang and X. N. Wang, Phys. Rev. Lett.94(2005), 102301 Erratum: [Phys. Rev. Lett.96(2006), 039901] [nucl-th/0410079].
- [6] F. Becattini, L. Csernai, D. J. Wang, Phys. Rev. C88 (2013) 034905
- [7] Mircea Baznat, Konstantin Gudima, Alexander Sorin, Oleg Teryaev, Phys. Rev. C 88, 061901 (2013)
- [8] M.I. Baznat, K.K. Gudima, A.S. Sorin, O.V. Teryaev, Phys. Rev. C 88, 061901 (2013)
- [9] S.A. Bass, M. Belkacem, M. Bleicher, M. Brandstetter, L. Bravina, C. Ernst, L. Gerland, M. Hofmann, S. Hofmann, J. Konopka, G. Mao, L. Neise, S. Soff, C. Spieles, H. Weber, L.A. Winckelmann, H. St ocker, W. Greiner, Ch. Hartnack, J. Aichelin, and N. Amelin, Prog. Part. Nucl. Phys.41, 225 (1998).
- [10] M. Bleicher, E. Zabrodin, C. Spieles, S.A. Bass, C. Ernst, S. Soff, L. Bravina, H. Weber, H. St ocker, and W. Greiner, J. Phys. G25(1999) (in press)
- [11] L.V. Bravina, E.E. Zabrodin, M.I. Gorenstein, S.A. Bass, M. Belkacem, M. Bleicher, M. Brandstetter, C. Ernst, M. Hofmann, L. Neise, S. Soff, H. Weber, H. Stoecker, W. Greiner, arXiv:hep-ph/9906548